

# Quinolactacins revisited: from lactams to imide and beyond

Ben Clark,<sup>a</sup> Robert J. Capon,<sup>\*a</sup> Ernest Lacey,<sup>b</sup> Shaun Tennant<sup>b</sup> and Jennifer H. Gill<sup>b</sup>

Received 20th January 2006, Accepted 22nd February 2006

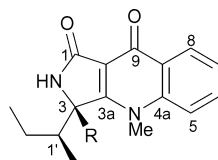
First published as an Advance Article on the web 16th March 2006

DOI: 10.1039/b600959j

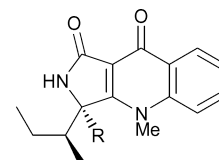
Chemical analysis of a solid phase fermentation of an Australian *Penicillium citrinum* strain has returned all known examples of a rare class of *N*-methyl quinolone lactams, quinolactacins A2 (**1**), B2 (**2**), C2 (**3**) and A1 (**4**), together with the new quinolactacins B1 (**5**), C1 (**6**), D1 (**7**) and D2 (**8**), and the novel derivatives quinolonimide (**9**) and quinolonic acid (**10**). Complete stereostructures were assigned to all these compounds by detailed spectroscopic analysis and chemical interconversion. Carefully controlled and monitored decomposition studies have confirmed that quinolactacins readily undergo C-3 epimerization and oxidation, and under appropriate conditions convert to quinolonimide and quinolonic acid. Mechanisms for key transformations are proposed. The decomposition studies suggested that only quinolactacins A2 (**1**) and B2 (**2**) are genuine natural products, with all other isolated compounds being decomposition artefacts. Quinolactacins C1 (**6**), C2 (**3**), and the racemic mixture of quinolactacins D1/D2 (**8/7**) all displayed notable cytotoxic activity.

## Introduction

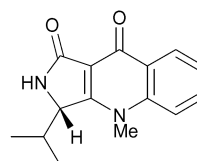
The quinolactacins are a rare class of fungal alkaloids that possess a unique *N*-methyl quinolone moiety fused to a lactam ring. The quinolactacins A2 (**1**), B2 (**2**) and C2 (**3**) were first reported by Takahashi *et al.* in 2000 from an unidentified *Penicillium* species.<sup>1,2</sup> At that time, the relative and absolute stereochemistry of the three quinolactacins were unknown and they were designated simply as quinolactacins A, B, and C, respectively. A subsequent report by Kim *et al.* in 2001<sup>3</sup> described two quinolactacin A epimers from a strain of *P. citrinum* Thom, and prompted revision of the nomenclature to distinguish these epimers as quinolactacin A1 (**4**) and A2 (**1**). Whereas Takahashi *et al.* described quinolactacin A2 (**1**) as an inhibitor of tumour necrosis factor (TNF) production in macrophages,<sup>1,2</sup> Kim *et al.* recognized **1** as an acetylcholinesterase inhibitor.<sup>3</sup> The structural novelty and biological activity of the quinolactacins prompted a biomimetic synthesis of quinolactacin B2 (**2**) in 2001<sup>4</sup> and an optimised synthesis of quinolactacins A1 (**4**), A2 (**1**) and B2 (**2**) in 2003.<sup>5</sup> As a result of the latter study, the absolute stereochemistry of **1** and **2** was unambiguously established, and determined to be consistent with the biosynthetic involvement of L-Ile and L-Val, respectively. This same study also concluded (incorrectly and without direct evidence) that quinolactacin A1 (**4**) was the C-1' epimer of quinolactacin A2 (**1**). If correct such a situation would necessitate the biosynthetic involvement of L-*allo*-Ile in the production of quinolactacin A1 (**4**). As will be demonstrated in this report, quinolactacins A1 and A2 are C-3 rather than C-1' epimers, and both are biosynthetically derived from L-Ile.



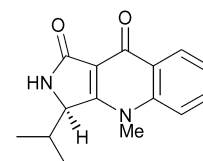
quinolactacin A2 (**1**) R = H  
quinolactacin C2 (**3**) R = OH



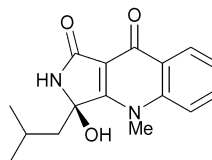
quinolactacin A1 (**4**) R = H  
quinolactacin C1 (**6**) R = OH



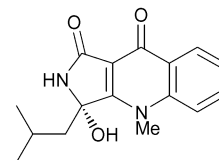
quinolactacin B2 (**2**)



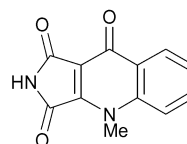
quinolactacin B1 (**5**)



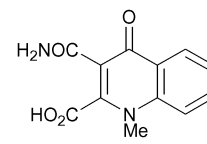
quinolactacin D2 (**7**)



quinolactacin D1 (**8**)



quinolonimide (**9**)



quinolonic acid (**10**)

<sup>a</sup>Centre for Molecular Biodiversity, Institute for Molecular Bioscience, University of Queensland, Brisbane, QLD 4072, Australia. E-mail: r.capon@imb.uq.edu.au; Fax: +61 7 3346 2090; Tel: +61 7 3346 2979

<sup>b</sup>Microbial Screening Technologies Pty Ltd, Smithfield, NSW 2164, Australia. E-mail: elacey@microbialscreening.com; Fax: +61 2 9757 4515; Tel: +61 2 9757 2586

As part of our research into the chemistry of Australian microorganisms we investigated a *P. citrinum* strain (MST-F10130) isolated from an Australian soil sample. The solid phase fermentation of this fungus led to the isolation and identification of the

known quinolactacins A2, B2, C2 and A1 (1–4), as well as the new quinolactacins B1 (5), C1 (6), D1 (7) and D2 (8), and the novel analogues quinolonimide (9) and quinolonic acid (10). Careful analysis of the quinolactacins revealed that all were unstable and engaged in a sequence of decomposition transformations that ultimately led to quinolonimide (9), and from there to quinolonic acid (10). To fully understand this hitherto undescribed aspect of quinolactacin chemistry we undertook a detailed study of the decomposition pathway. This study suggested that only quinolactacins A2 (1) and B2 (2) are genuine natural products, with all other “related co-metabolites” being decomposition artefacts.

## Results and discussion

The MeOH extract derived from a solid fermentation of *P. citrinum* (MST-F10130) was concentrated *in vacuo* and the residue fractionated by repeated reverse phase SPE and HPLC to yield the known *P. citrinum* metabolites, quinolactacins 1–4, together with the new quinolactacins B1 (5), C1 (6), D1 (7) and D2 (8), and the novel derivatives quinolonimide (9) and quinolonic acid (10).

Quinolactacin C1 (6) was isolated as a white solid that returned a HRESI(+)MS pseudomolecular ion ( $m/z$  309.1215,  $M + Na$ ) corresponding to a molecular formula ( $C_{16}H_{18}N_2O_3$ ) isomeric with quinolactacin C2 (3). The  $^1H$  NMR data for 6 was very similar to that for 3, with the only significant difference being a reversal in the relative chemical shifts of the 1° and 2° methyls (see Table 1). This data suggested that quinolactacins C1 (6) was an epimer of quinolactacin C2 (3), much as quinolactacin A1 (4) was to quinolactacin A2 (1). Full NMR data for 3 and 6 are given in Tables 1 and 2.

The relative stereochemistry about the chiral centres C-3 and C-1' in 3 and 6 was confirmed by NOESY experiments and molecular modelling studies. A NOESY experiment carried out on 6 displayed correlations between H-2' and the amide proton H-2, and between the N4-Me and H-1'. By contrast, NOESY data for 3 revealed key correlations from the 1'-Me to H-2, and from H-1' to the N4-Me. Consistent with the NOESY data, molecular modelling studies (MM2) suggested that the lowest energy conformation of both 3 and 6 around the C-1' to C-3 bond were those indicated in Fig. 1, with H-1' oriented towards the 4-Me. The absolute configurations of 3 and 6 were not determined at this time, however, as will be discussed later in this report, the absolute stereochemistry is as indicated.

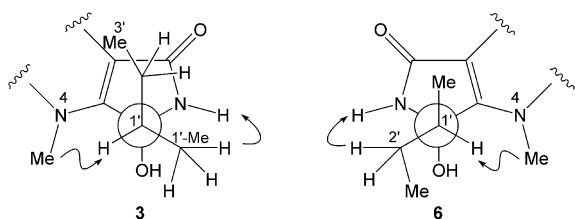


**Fig. 1** Key NOESY correlations used to determine the relative stereochemistry in quinolactacins C1 (6) and C2 (3).

Quinolactacin D, initially believed to be a single compound, was isolated as a white solid that returned a HRESI(+)MS

**Table 1**  $^1H$  NMR and selected gHMBC data for compounds 6–10 (600 MHz,  $d_6$ -DMSO)

	6		7/8		9		10	
	$\delta_H$	gHMBC <sup>a</sup>	$\delta_H$	gHMBC <sup>a</sup>	$\delta_H$	gHMBC <sup>a</sup>	$\delta_H$	gHMBC <sup>a</sup>
H-2	8.21 (s)	C-1, C-3, C-3a, C-9a	8.30 (s)		11.31 (s)	C-3, C-3a, C-9a	9.46 (s), 6.92 (s)	
H-5	7.87 (d, 8.5)	C-7, C-8a	7.87 (d, 8.4)		8.02 (d, 8.8)	C-6, C-7/8, C-8a, C-9	7.79 (m) <sup>c</sup>	
H-6	7.83 (ddd, 8.5, 6.9, 1.6)	C-4a, C-8	7.82 (ddd, 8.4, 6.8, 1.7)		7.90 (ddd, 1.8, 7.0, 8.8)	C-4a, C-5, C-7/8	7.77 (m) <sup>c</sup>	
H-7	7.50 (ddd, 7.9, 6.9, 1.1)	C-5, C-8a	7.50 (ddd, 8.0, 6.8, 1.1)		7.59 (ddd, 0.7, 7.0, 8.0)	C-5, C-6, C-7/8, C-8a	7.46 (ddd, 2.5, 5.6, 8.3)	
H-8	8.25 (dd, 7.9, 1.6)	C-4a, C-6, C-9	8.25 (dd, 8.0, 1.7)		8.29 (dd (1.8, 8.0))	C-4a, C-6, C-9	8.27 (d, 8.3)	
N4-Me	4.02 (s)	C-3a, C-4a	4.02 (s)		4.23 (s)	C-3a, C-4a, C-5	3.82 (s)	
3-OH	6.92 (s)		6.87 (brs)					
1'	2.19 (m)	C-3, C-2'	2.06 (dd, 14.5, 6.7)					
2'	2.01 (m)		2.01 (dd, 14.6, 5.6)					
3'	1.15 (m)	C-1', C-3', 1'-Me	1.44 (m)					
1'-Me	0.95 (t, 7.5)	C-1', C-3', 1'-Me	0.88 (d, 6.7)					
2'-Me	0.54 (d, 6.7)	C-1', C-2'	0.58 (d, 6.6)					

<sup>a</sup>gHMBC correlations for 7/8 were very similar to those of 6. <sup>b</sup>gHMBC correlations for 10 were very similar to those of 9, though no correlations were observed from amide protons of 10. <sup>c</sup>Difficulty in determining multiplicity and gHMBC correlations due to overlapping signals.

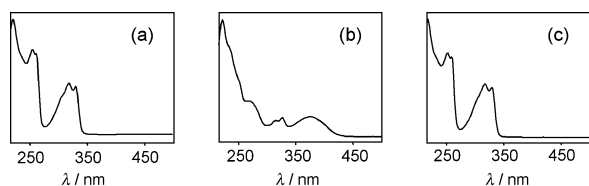
**Table 2**  $^{13}\text{C}$  NMR data (150 MHz,  $d_6$ -DMSO) for compounds **6–10**<sup>a</sup>

	<b>6</b>	<b>7/8</b>	<b>9</b>	<b>10</b> <sup>b</sup>
C-1	166.4	165.8	166.8 <sup>c</sup>	166.5 <sup>c</sup>
C-3	88.4	85.7	165.9 <sup>c</sup>	165.2 <sup>c</sup>
C-3a	163.4	162.9	146.9	160.5
C-4a	141.4	141.2	141.9	139.7
C-5	117.2	117.1	118.7	117.1
C-6	132.7	132.7	133.9	132.5
C-7	124.6	124.7	126.4	124.1
C-8	125.8	125.8	126.4	125.8
C-8a	128.5	128.5	130.7	125.9
C-9	171.5	171.5	171.2	176.0
C-9a	108.8	108.6	108.2	106.3
N4-Me	34.5	34.5	33.7	37.0
C-1'	40.9	45.9		
C-2'	22.4	23.8		
C-3'	12.4	23.7		
1'-Me	13.1			
2'-Me		22.8		

<sup>a</sup> All assignments assisted by gHMBC, gHSQC experiments. <sup>b</sup>  $^{13}\text{C}$  NMR data for **10** at 183 MHz.  $\delta_{\text{N}}$  105.9 for N-2 of **10**. Taken from  $^1\text{H}$ - $^{15}\text{N}$  gHSQC, at 750 MHz. Value referenced to nitromethane at 379.5 ppm. <sup>c</sup> Values within a column may be interchanged.

pseudomolecular ion ( $m/z$  309.1213,  $\text{M} + \text{Na}$ ) corresponding to a molecular formula ( $\text{C}_{16}\text{H}_{18}\text{N}_2\text{O}_3$ ) isomeric with both quinolactacins C1 (**6**) and C2 (**3**). The  $^1\text{H}$  NMR data for quinolactacin D was very similar to that for **3**, with differences restricted to the sidechain—which featured two doublet methyls—suggestive of replacement of the *sec*-butyl side-chain in **3** with an isobutyl side-chain for quinolactacin D. This analysis was subsequently confirmed by 2D NMR analysis. As described above for quinolactacin B1 and B2, it proved very difficult to secure a meaningful  $[\alpha]_{\text{D}}$  measurement for quinolactacin D, leading to speculation that quinolactacin D may exist as a racemate (or be racemizing). Chiral HPLC analysis and degradation studies, discussed in detail below, confirmed that this was indeed the case, leading to the revised nomenclature of quinolactacins D1 (**8**) and D2 (**7**). These subsequent studies also confirmed the absolute stereochemistry as shown.

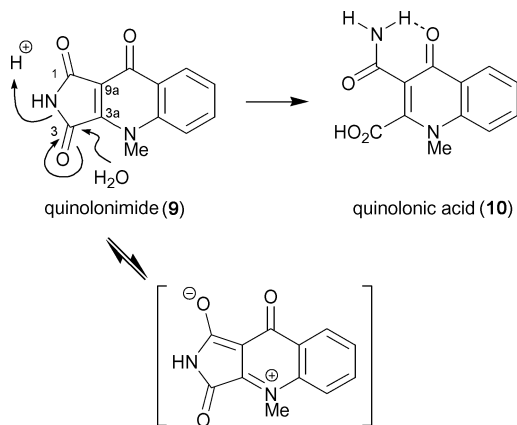
During the isolation of the quinolactacins a minor “co-metabolite” was detected. Quinolonimide (**9**) was particularly noteworthy in that it possessed a distinctive UV-vis spectrum (Fig. 2) that differed significantly from that of a typical quinolactacin. Curiously, during reverse phase HPLC **9** rapidly hydrolysed to a more polar compound, quinolonic acid (**10**), that displayed a more typical “quinolactacin” UV-vis spectrum (Fig. 2). This irreversible addition of  $\text{H}_2\text{O}$ , confirmed by LC-DAD-MS, led to speculation that, despite the differing UV-vis spectrum, **9** did indeed belong to the quinolactacin family but was undergoing

**Fig. 2** UV-vis spectra of (a) quinolactacins, (b) quinolonimide (**9**) and (c) quinolonic acid (**10**).

a clean hydrolysis to yield **10** on exposure to the acidic (0.01% TFA) HPLC conditions. Thus, a second attempt at purification with reduced exposure to acid led to the successful isolation of quinolonimide (**9**).

Quinolonimide (**9**) was isolated as a yellow solid that returned a HRESI(+)-MS pseudomolecular ion ( $m/z$  251.0429,  $\text{M} + \text{Na}^+$ ) corresponding with a molecular formula ( $\text{C}_{12}\text{H}_8\text{N}_2\text{O}_3$ ) requiring 10 double bond equivalents (DBE). Examination of the  $^1\text{H}$  NMR spectrum of **9** revealed resonances attributable to the “quinolactacin” *N*-methyl quinolone moiety (*i.e.* four contiguous aromatic protons and an *N*-methyl). A gHMBC analysis (Table 1) further confirmed the presence of the “quinolactacin” *N*-methyl quinolone moiety. The two remaining unassigned carbon resonances ( $\delta_{\text{C}}$  166.5 and 165.3) were attributed to  $\text{sp}^2$  ester/amide carbonyls. These, together with a broad deshielded exchangeable proton ( $\delta_{\text{H}}$  11.31), and a single remaining DBE, suggested that quinolonimide (**9**) incorporated a fused imide ring as indicated. A series of gHMBC correlations from the imide NH to C-3, C-3a and C-9a further supported the assigned structure, while extended conjugation from the *N*-methyl quinolone to the imide explained changes in the UV-vis spectrum of **9** relative to quinolactacins (Fig. 2). Finally, hydrolysis of the imide provided an explanation for the acid instability of **9**, and formation of quinolonic acid (**10**).

Quinolonic acid (**10**), recovered as a white solid, returned a HRESI(+)-MS pseudomolecular ion ( $m/z$  247.0714,  $\text{M} + \text{Na}$ ) consistent with a molecular formula ( $\text{C}_{12}\text{H}_{10}\text{N}_2\text{O}_4$ ) corresponding to the addition of  $\text{H}_2\text{O}$  to quinolonimide (**9**). Although in principle the hydrolysis of **9** could occur *via*  $\text{H}_2\text{O}$  attack at either C-1 or C-3, leading to two isomeric hydrolysis products, in practice the resonance structure indicated in Fig. 3 deactivated C-1 with respect to nucleophilic attack, and ensured that the hydrolysis process was regioselective. Specificity was established experimentally from the appearance of only a single peak in the LC-DAD-MS of **10**, and the absence of any peak doubling in the  $^1\text{H}$  NMR spectrum. Analysis of the  $^1\text{H}$  and  $^{13}\text{C}$  NMR data (Tables 1 and 2) for **10** confirmed the presence of an intact *N*-methyl quinolone unit, while a  $^1\text{H}$ - $^{15}\text{N}$  gHSQC experiment revealed that two broad exchangeable proton resonances were associated with a common primary amide nitrogen ( $\delta_{\text{N}}$  105.9). The strongly deshielded nature

**Fig. 3** Regiospecific hydrolysis of quinolonimide (**9**) to quinolonic acid (**10**). The resonance form as shown reduces the susceptibility of C-1 to nucleophilic attack, and directs hydrolysis to C-3.

of one of these amide protons ( $\delta_{\text{H}}$  9.46) relative to the other ( $\delta_{\text{H}}$  6.92) was characteristic of a hydrogen-bonded amide proton, implying that the amide moiety was adjacent to the quinolone carbonyl as proposed (see Fig. 3). Literature data for an analogous system gave similar  $^1\text{H}$  NMR amide proton chemical shifts.<sup>6</sup> Likewise, literature reports on the regiospecific hydrolysis of imides incorporating a C-4 nitrogen substituent<sup>7,8</sup> provided supporting evidence for the proposed structure assignments. To confirm that quinolonic acid (**10**) was indeed a hydrolysis product, a small sample of pure quinolonimide (**9**) was heated in an acidic, aqueous environment. After two days, LC-DAD-MS analysis showed quantitative conversion to **10**.

### Decompositions and stereochemical studies

Ongoing LC-DAD-MS and  $^1\text{H}$  NMR monitoring of the integrity of purified quinolactacins during handling and storage revealed an unexpected observation. During handling and storage pure samples of both **4** and **1** underwent slow epimerization such that each sample became contaminated with the other. On further handling and storage each of these mixtures accumulated small quantities of quinolactacins C1 (**6**) and C2 (**3**). While it was possible that this effect was due to cross-contamination during handling, it seemed more probable that the quinolactacins were in fact slowly interconverting over time. To test this hypothesis a range of decomposition experiments were carried out.

Triplicate samples (0.2 mg) of pure **1** and **4** were dissolved in (i) DMSO (0.5 mL) (ii) MeOH (0.5 mL) plus a drop of triethylamine (TEA) and (iii) MeOH (0.5 mL) plus a drop of trifluoroacetic acid (TFA). Care was taken to keep all samples at room temperature ( $rt = 25\text{ }^\circ\text{C}$ ) or below. Condition (i) was designed to emulate the drying of samples after NMR and  $[a]_{\text{D}}$  analyses, while (ii) and (iii) were designed to mimic conditions encountered during fractionation. All samples were allowed to stand at  $rt$  for 24 h, and then heated to  $50\text{ }^\circ\text{C}$  for a further 7 d. Reaction progress was monitored throughout by LC-DAD. Unfortunately, a single HPLC method could not be devised to simultaneously differentiate between **1**, **3**, **4** and **6**, thus two HPLC methods were employed. The first method (left window in Fig. 4) used a Zorbax Eclipse-C<sub>8</sub> column to differentiate between **1** and **4**, while the second method (right window in Fig. 4) used a Zorbax StableBond-Phenyl column to differentiate between **3** and **6**. Selected LC-DAD analyses are shown in Fig. 4.

Under neutral conditions (i) the decomposition of quinolactacins A2 (**1**) (Fig. 4a) and A1 (**4**) (Fig. 4b) proceeded slowly at  $rt$ , but rapidly on heating, to a mixture of quinolactacins C1 (**6**) and C2 (**3**) after 7 d.

Under acidic conditions (ii) the decomposition of quinolactacin A1 (**4**) (Fig. 4c) proceeded at  $rt$  to the epimer **1**, then on heating to quinolactacin C1 and C2 (**6** and **3**) plus quinolonimide (**9**) and a pair of unidentified compounds **11** and **12**. Although not isolated, LC-DAD-MS analysis of **11** and **12** revealed them to be isomeric with pseudomolecular ions ( $m/z$  323,  $M + \text{Na}$ ) corresponding to a molecular weight 14 amu heavier than **6** and **3**. A possible explanation is that **11** and **12** are the methoxylated quinolactacins as shown, formed by methanolysis of **6** and **3**. The acid mediated decomposition of quinolactacin A2 (**1**) (not shown) led to a similar outcome.

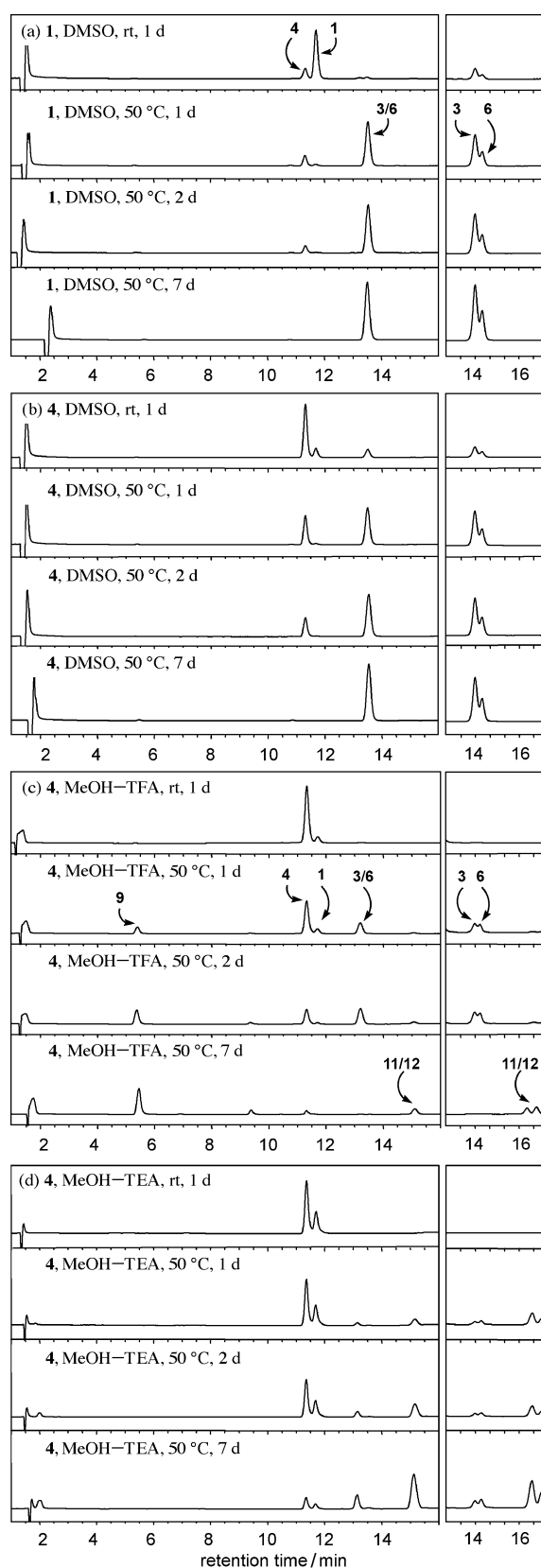
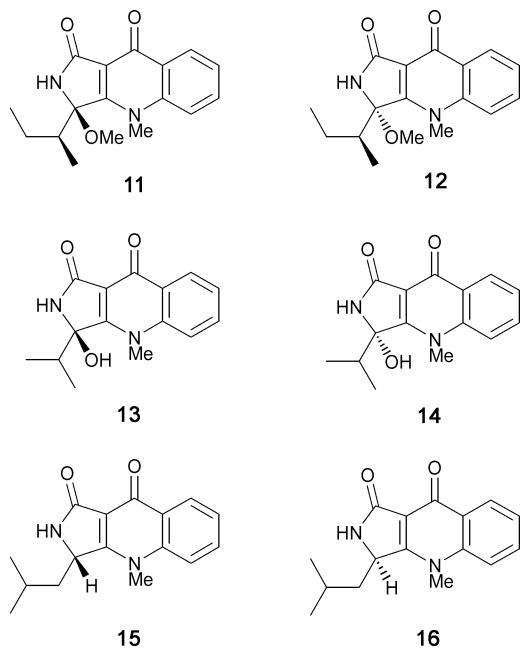


**Fig. 4** Decomposition of quinolactacins A1 (**4**) and A2 (**1**) under various conditions. LC-DAD analysis using a Zorbax Eclipse-C<sub>8</sub> column (left window) and a Zorbax StableBond-Ph column (right window). DAD traces were extracted at 320 nm.

Under basic conditions (iii) the decomposition of quinolactacin A1 (**4**) (Fig. 4d) proceeded rapidly at rt to return an equilibrium mixture of **4** and **1**, which on heating was converted to **6**, **3**, **11** and **12**. Of note, quinolactacin A1 (**4**) was not transformed into quinolonimide (**9**) under basic conditions. The base mediated decomposition of quinolactacin A2 (**1**) (not shown in Fig. 4) led to similar outcomes.



In light of the decomposition observations described above it was anticipated that the samples of quinolactacins B and D encountered during this study were rendered racemic during handling and storage. To confirm this hypothesis freshly purified samples of “quinolactacins B and D”, that eluted as single peaks under standard HPLC conditions, were subjected to chiral HPLC analysis. These studies clearly resolved quinolactacins B1 (**5**) from B2 (**2**), as well as D1 (**8**) from D2 (**7**). The absolute stereochemistry of **5** and **2** were assigned based on the published synthesis,<sup>5</sup> which required that **2** be the natural product derived from L-Val, and **5** be the epimerized artifact. Nomenclature for the quinolactacins D1 (**8**) and D2 (**7**) enantiomers followed this same reasoning.

The potential mechanism for the epimerization of quinolactacins as shown in Fig. 5 would operate under neutral conditions in a protic solvent (*i.e.* MeOH), but would be accelerated under basic conditions—as observed experimentally (see Fig. 4). This mechanism suggests that quinolactacins A1 (**4**) and B1 (**5**) are C-3 epimer artefacts of the natural products quinolactacins A2 (**1**) and B2 (**2**), and all are biosynthetically related to L-amino acids. While not indicating a preferred mechanism for the C-3 oxidative conversion of quinolactacins A1 (**4**) and A2 (**1**) into quinolactacins C1 (**6**) and C2 (**3**), we note that C-3 is “activated” to oxidation. Although not directly isolated during this study, controlled decomposition of quinolactacins B1 (**5**) and B2 (**2**), under conditions as outlined above, resulted in conversion to oxidized products suggestive of **13** and **14**, as determined by LC-DAD-MS analysis. Likewise, quinolactacins D1 (**8**) and D2 (**7**) are in all probability the artifact oxidation products of the undetected precursors **15** and **16**, of which **16** might be expected to be the artifact epimer of the hypothetical natural product **15**.

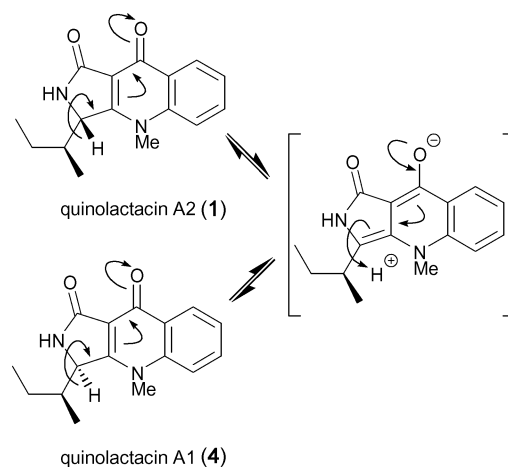


**Fig. 5** Proposed mechanisms for the C-3 epimerisation of quinolactacins A1 (**4**) and A2 (**1**).

A tentative mechanism for the formation of quinolonimide (**9**) is proposed in Fig. 6. As confirmed experimentally (see Fig. 4), this mechanism is acid mediated. It is proposed that the reaction proceeds *via* an acid-initiated elimination of H<sub>2</sub>O and subsequent rearrangement to yield the substituted acylated enamine intermediate shown. This unstable intermediate might be expected to undergo oxidation to yield **9**.

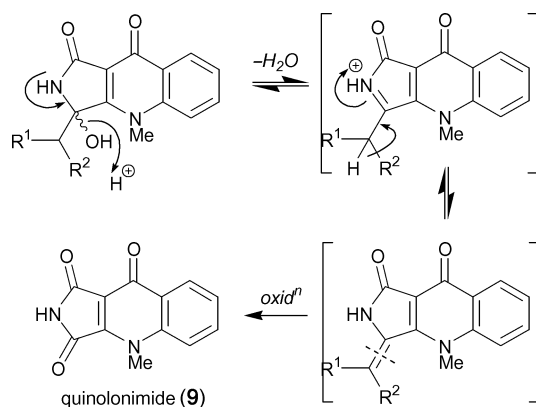


**Fig. 6** Proposed mechanisms for the formation of quinolonimide (**9**).

In light of these results and mechanistic speculations, an overall scheme can be formulated for the stepwise decomposition of the quinolactacins (Fig. 7), with quinolactacin A2 (**1**) used as a representative example. Careful manipulation of reaction conditions could be used to give any of the products shown in good yield.

The quinolactacins, quinolonimide and quinolonic acid isolated in this study were assayed for antimicrobial activity against a number of microorganisms, and for cytotoxic activity against the mouse NS-1 cell line. No antimicrobial activity was observed, however, quinolactacins C1 (**6**), C2 (**3**) and the racemic mixture of quinolactacins D1/D2 (**8/7**) displayed notable cytotoxic activity in the NS-1 bioassay (LD<sub>99</sub> = 40, 40, and 7.5 μg mL<sup>-1</sup>, respectively).

Ongoing biological evaluation of the quinolactacins and their decomposition products is directed at their impact on TNFα production and acetylcholinesterase, and their differential cytotoxicity against a panel of human cancer cell lines. To support these

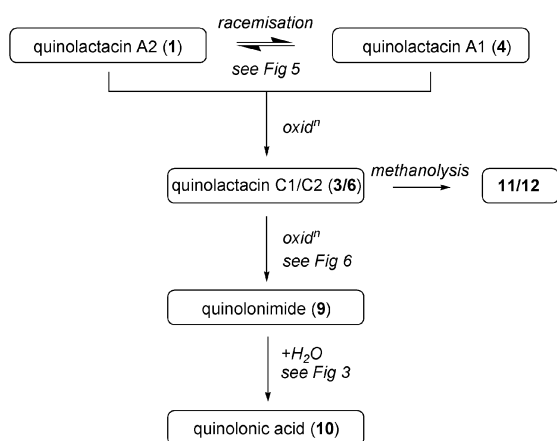


**Fig. 7** Overall scheme for the decomposition of quinolactacin A2 (1). Analogous schemes can be proposed for the decomposition of quinolactacin B2 (2) and the hypothetical quinolactacin D precursor 15.

studies we are also exploring the total synthesis of quinolonimide and quinolonic acid. The results from these ongoing studies will be reported at a future date.

## Experimental

Chemicals were purchased from Merck, Sigma, Aldrich or Fluka. Solvents were at least analytical grade. Solvents used for HPLC were HPLC grade, and were filtered through an Alltech 0.45  $\mu\text{m}$  polytetrafluoroethylene filter before use. Water for HPLC use was filtered through either a Millipore filtration system or an ELGA Purelab Ultra system. Molecular modelling was carried out using the MM2 algorithm, using CambridgeSoft Chem3D Pro v7.0 unless otherwise specified. Substructure searches were carried out using both Antibase 2002<sup>9</sup> and Scifinder Scholar 2004.

Chiroptical measurements ( $[\alpha]_D$ ) were obtained on a Jasco P-1010 intelligent remote module type polarimeter, in a 100 by 2 mm cell, at 22 °C, unless otherwise specified. Optical rotations were recorded at the sodium D line (589 nm) with values reported in  $\text{deg mL g}^{-1} \text{dm}^{-1}$ , and concentrations in g per 100 mL. Circular dichroism (CD) spectra were acquired using a JASCO J-810 spectropolarimeter, and a 1 mm quartz cell. Ultraviolet-visible (UV-vis) absorption spectra were obtained using a CARY3 UV-visible spectrophotometer with 1 cm quartz cells. Infrared (IR) spectra were acquired using a Jasco FT/IR-460 Plus spectrometer, with samples examined in a NaCl solution cell.  $^1\text{H}$  and  $^{13}\text{C}$  NMR spectra were acquired on a Bruker Avance 500, a Bruker Avance 600, or a Bruker Avance 750 spectrometer under XWIN-NMR control. Solvents are as indicated in the text and signals were referenced to residual  $^1\text{H}$  signals in the deuterated solvents. Electrospray ionisation mass spectra (ESIMS), both flow injection analysis (FIA) and liquid chromatography-diode array-mass spectrometry (LC-DAD-MS), were acquired using an Agilent 1100 series separations module equipped with an Agilent 1100 series LC/MSD mass detector and Agilent 1100 series diode array. High-resolution (HR) ESIMS measurements were obtained on a Finnigan MAT 900 XL-Trap instrument with a Finnigan API III source.

HPLC was performed using the following two basic system types: (1) Agilent 1100 Series separations module equipped with a six column switching capability (where necessary), Agilent 1100 Series diode array, Polymer Laboratories PL-ELS1000 ELSD and Agilent 1100 Series fraction collector and running ChemStation (Revisions 9.03A or 10.0A) software or (2) two Shimadzu LC-8A preparative liquid chromatographs with static mixer, Shimadzu SPD-M10AVP diode array detector and Shimadzu SCL-10AVP system controller.

## Analytical HPLC gradients

Standard LC-DAD-MS analyses were carried out using the following gradient: 1  $\text{mL min}^{-1}$  gradient elution from 90%  $\text{H}_2\text{O}$ -MeCN (0.05%  $\text{HCO}_2\text{H}$ ) to MeCN (0.05%  $\text{HCO}_2\text{H}$ ) using a 5  $\mu\text{m}$  Zorbax StableBond  $\text{C}_8$  150  $\times$  4.6 mm column.

The decomposition of the quinolactacins was monitored using the following gradient: 1  $\text{mL min}^{-1}$  gradient elution from 75 to 50%  $\text{H}_2\text{O}$ -MeOH using either (a) a 5  $\mu\text{m}$  Zorbax Eclipse XDB- $\text{C}_8$  150  $\times$  4.6 mm column or (b) a 5  $\mu\text{m}$  Zorbax StableBond Phenyl 150  $\times$  4.6 mm column. Condition (a) was used to separate quinolactacins A1 (4) and A2 (1), while (b) was used to separate quinolactacins C1 (6) and C2 (3).

Chiral LC-DAD-MS analyses of 2/5 and 7/8 were carried out using a 1  $\text{mL min}^{-1}$  isocratic elution using 70%  $\text{H}_2\text{O}$ -MeOH, through a 5  $\mu\text{m}$  Astec Chirobiotic T 4.6  $\times$  150 mm column. Integrations were taken at 320 nm.

## Assays

Details for antimicrobial and cytotoxicity assays have been given previously.<sup>10</sup>

## Biological material

The fungal strain (MST-F10130) was isolated from a roadside soil sample collected near Ardlethan in New South Wales, Australia. The isolate was identified as *Penicillium citrinum* Thom on morphological grounds.

## Isolation

A solid fermentation (1 kg wheat, 21 d, 28 °C) was extracted twice with MeOH (ca. 6 L). These extracts were combined and concentrated *in vacuo* to an aqueous concentrate (2 L) and triethylamine added to adjust to pH ca. 8.5. This solution was passed through four parallel  $\text{C}_{18}$  SPE cartridges (4  $\times$  10 g, Varian HF  $\text{C}_{18}$ ) followed by sequential elution with 50%  $\text{H}_2\text{O}$ -MeOH (4  $\times$  40 mL each) and MeOH (4  $\times$  40 mL each). The aqueous eluant was adjusted to pH ca. 3.5 with the addition of trifluoroacetic acid (TFA) and passed through the same  $\text{C}_{18}$  SPE cartridges followed by similar sequential elution to afford 50%  $\text{H}_2\text{O}$ -MeOH and MeOH fractions. All 50%  $\text{H}_2\text{O}$ -MeOH and MeOH eluants were concentrated *in vacuo* to give a combined residue (ca. 7.9 g). This residue was equally divided and subjected to preparative HPLC (five injections, 60  $\text{mL min}^{-1}$  with gradient elution of 70 to 40%  $\text{H}_2\text{O}$ -MeCN (0.01% TFA) over 20 min followed by MeCN (0.01% TFA) for 10 min, through a 5 mm Phenomenex Luna  $\text{C}_{18(2)}$  50  $\times$  100 mm column, giving 100 fractions. These were pooled based on HPLC analysis to give 10 combined fractions.

The fractions richest in quinolactacins (based on analytical HPLC analysis) were pooled and evaporated to afford a combined residue (916 mg). This was re-subjected to preparative HPLC (single injection, 60 mL min<sup>-1</sup> with isocratic elution of 79% H<sub>2</sub>O–MeCN (0.01% TFA) over 30 min, through a 5 μm Phenomenex Luna C<sub>18(2)</sub> 50 × 100 mm column), giving an additional 13 fractions.

Several of the more polar of these 13 fractions were further fractionated by repeated reversed phase HPLC (3 mL min<sup>-1</sup> gradient elution from 90 to 50% H<sub>2</sub>O–MeCN over 20 min, through a 5 μm Zorbax StableBond C<sub>8</sub> 9.4 × 250 mm column, followed by another gradient from 95 to 68% H<sub>2</sub>O–MeCN (0.01% TFA) over 20 min, through a 5 μm Zorbax StableBond Aqua 9.4 × 150 mm column) to yield a mixture of quinolactacin B1/B2 (2/5) (0.6 mg), and a mixture containing both quinolonimide (9) and quinolonic acid (10). A subsequent attempt to purify the latter mixture by the same method led to the decomposition of 9 and yielded only 10 (1.4 mg). Preparative C<sub>18</sub> HPLC of another fraction (16 mL min<sup>-1</sup> isocratic elution using 65% H<sub>2</sub>O–MeOH, through a 5 μm Zorbax StableBond C<sub>18</sub> 21.2 × 250 mm column) gave additional quantities of quinolonimide (9) (3.2 mg) and a 1 : 1 mixture of quinolactacins A1 (4) and A2 (1). A portion of this epimeric mixture (15 mg) was separated by HPLC (3.2 mL min<sup>-1</sup> isocratic elution using 70% H<sub>2</sub>O–MeOH, through a 5 μm Zorbax Eclipse C<sub>18</sub> 9.4 × 250 mm column) to yield pure quinolactacins A1 (4) and A2 (1) (6.2 and 5.8 mg, respectively).

Less polar quinolactacin containing fractions were also separated by repeated reverse phase HPLC (3 mL min<sup>-1</sup> isocratic elution with 64% H<sub>2</sub>O–MeOH for 40 min, through a 5 μm Zorbax Stablebond Phenyl-hexyl 9.4 × 250 mm column and then 68% H<sub>2</sub>O–MeOH isocratic elution for 25 min through a 4 μm Phenomenex Synergi Fusion-RP 4.6 × 150 mm column) yielding quinolactacins C1 (6) (2.7 mg), C2 (3) (2.4 mg) and D1/D2 (7/8) (1.6 mg).

**Quinolactacin A2 (1).** Identified by spectroscopic analysis (ESI(±)MS, HRESI(+)MS, [ $\alpha$ ]<sub>D</sub>, CD, UV-vis, <sup>1</sup>H, <sup>13</sup>C and 2D NMR) and comparison with literature values.<sup>1,3</sup>

**Quinolactacin B1/B2 (5/2).** Identified by spectroscopic analysis (ESI(±)MS, HRESI(+)MS, UV-vis, <sup>1</sup>H, <sup>13</sup>C and 2D NMR) and comparison with literature values.<sup>1</sup> No [ $\alpha$ ]<sub>D</sub> value could be obtained due to the presence of a racemic mixture.

**Quinolactacin C2 (3).** Identified by spectroscopic analysis (ESI(±)MS, HRESI(+)MS, UV-vis, [ $\alpha$ ]<sub>D</sub>, <sup>1</sup>H, <sup>13</sup>C and 2D NMR) and comparison with literature values.<sup>1</sup>

**Quinolactacin A1 (4).** Identified by spectroscopic analysis (ESI(±)MS, HRESI(+)MS, CD, UV-vis, <sup>1</sup>H, <sup>13</sup>C and 2D NMR) and comparison with literature values.<sup>3</sup> An [ $\alpha$ ]<sub>D</sub> value was recorded for the first time: +30.3° (*c* 0.16, DMSO).

**Quinolactacin C1 (6).** White solid; [ $\alpha$ ]<sub>D</sub> +39.6° (*c* 0.12, DMSO); IR  $\nu_{\max}$ (CHCl<sub>3</sub>)/cm<sup>-1</sup> 3226, 2968, 2930, 1697, 1607, 1523; UV-vis  $\lambda_{\max}$ (MeOH) 328 ( $\epsilon$ /dm<sup>3</sup>mol<sup>-1</sup>cm<sup>-1</sup> 8900), 315 (9000), 304 (sh) (10100), 259 (13400), 250 (13900), 216 (24800) nm; <sup>1</sup>H NMR (d<sub>6</sub>-DMSO; 600 MHz) see Table 1; <sup>13</sup>C NMR (d<sub>6</sub>-DMSO; 150 MHz) see Table 2; ESI(+)MS *m/z* 595 (2M + Na), 287 (M + H); HRESI(+)MS *m/z* 309.1215 (M + Na, C<sub>16</sub>H<sub>18</sub>N<sub>2</sub>O<sub>3</sub>Na, requires 309.1215).

**Quinolactacin D1/D2 (8/7).** White solid; IR  $\nu_{\max}$ (CHCl<sub>3</sub>)/cm<sup>-1</sup> 3226, 2959, 2929, 1699, 1608, 1522, 1465, 1420; UV-vis  $\lambda_{\max}$ (MeOH) 329 ( $\epsilon$ /dm<sup>3</sup>mol<sup>-1</sup>cm<sup>-1</sup> 8000), 315 (8200), 259 (12100), 250 (12600), 216 (23100) nm; <sup>1</sup>H NMR (d<sub>6</sub>-DMSO; 600 MHz) see Table 1; <sup>13</sup>C NMR (d<sub>6</sub>-DMSO; 150 MHz) see Table 2; ESI(+)MS *m/z* 595 (2M + Na), 309 (M + Na); HRESI(+)MS *m/z* 309.1213 (M + Na, C<sub>16</sub>H<sub>18</sub>N<sub>2</sub>O<sub>3</sub>Na requires 309.1215). No [ $\alpha$ ]<sub>D</sub> value could be obtained due to the presence of a racemic mixture.

**Quinolonimide (9).** Pale yellow solid; UV-vis  $\lambda_{\max}$ (MeOH) 371 ( $\epsilon$ /dm<sup>3</sup>mol<sup>-1</sup>cm<sup>-1</sup> 2700), 325 (4300), 313 (3800), 269 (sh) (5600), 251 (sh) (8700), 224 (12500); <sup>1</sup>H NMR (d<sub>6</sub>-DMSO; 600 MHz) see Table 1; <sup>13</sup>C NMR (d<sub>6</sub>-DMSO; 150 MHz) see Table 2; ESI(+)MS *m/z* 479 (2M + Na), 229 (M + H). HRESI(+)MS *m/z* 251.0429 (M + Na, C<sub>12</sub>H<sub>8</sub>N<sub>2</sub>O<sub>3</sub>Na requires 251.0433).

**Quinolonic acid (10).** White solid; UV-vis  $\lambda_{\max}$ (MeOH) 329 ( $\epsilon$ /dm<sup>3</sup>mol<sup>-1</sup>cm<sup>-1</sup> 3400), 316 (4000), 304 (sh) (3500), 258 (8500), 250 (8600), 221 (9300); <sup>1</sup>H NMR (d<sub>6</sub>-DMSO; 600 MHz) see Table 1; <sup>13</sup>C NMR (d<sub>6</sub>-DMSO; 187 MHz) see Table 2; ESI(+)MS *m/z* 247 (M + H); ESI(-)MS 245 (M-H), 201 (M - CO<sub>2</sub>-H); HRESI(+)MS *m/z* 247.0714 (M + H, C<sub>12</sub>H<sub>11</sub>N<sub>2</sub>O<sub>4</sub> requires 247.0719).

#### Hydrolysis of quinolonimide (9)

Quinolonimide (9, 0.1 mg) was dissolved in H<sub>2</sub>O–DMSO–TFA (4 : 1 : 0.1) and heated at 50 °C for 2 d. After this time, LC-DAD-MS analysis revealed that full conversion to quinolonic acid (10) had occurred. A similar reaction using MeOH–DMSO–TFA (4 : 1 : 0.1) gave no reaction after 2 d.

#### Decomposition studies

Fresh samples of pure quinolactacins A1 (4) and A2 (1) were split into three equal samples (*ca.* 0.2 mg). For both 4 and 1, one sample was dissolved in DMSO (0.5 mL), a second in MeOH (0.5 mL) with a drop of TFA added, and a third in MeOH with a drop of TEA added. All samples were left at room temperature for 1 d, and then heated at 50 °C for a further week, with progress monitored by LC-DAD analysis. Where unknown species were detected, the samples were re-analysed by LC-DAD-MS analysis, using the same gradients.

#### Acknowledgements

The authors would like to acknowledge A. Hocking for taxonomic studies, G. MacFarlane for acquisition of HRESI(+)MS data, and L. Lambert for assistance with 750 MHz NMR studies. This research was partially funded by the Australian Research Council.

#### References

- 1 S. Takahashi, N. Kakinuma, H. Iwai, T. Yanagisawa, K. Nagai, K. Suzuki, T. Tokunaga and A. Nakagawa, *J. Antibiot.*, 2000, **53**, 1252–1256.
- 2 N. Kakinuma, H. Iwai, S. Takahashi, K. Hamano, T. Yanagisawa, K. Nagai, K. Tanaka, K. Suzuki, F. Kirikae, T. Kirikae and A. Nakagawa, *J. Antibiot.*, 2000, **53**, 1247–1251.
- 3 W.-G. Kim, N.-K. Song and I.-D. Yoo, *J. Antibiot.*, 2001, **54**, 831–835.

- 
- 4 K. Tatsuta, H. Misawa and K. Chikauchi, *J. Antibiot.*, 2001, **54**, 109–112.
  - 5 X. Zhang, W. Jiang and Z. Sui, *J. Org. Chem.*, 2003, **68**, 4523–4526.
  - 6 G. Tennant, C. J. Wallis and G. W. Weaver, *J. Chem. Soc., Perkin Trans. 1*, 1999, 827–832.
  - 7 J. R. Beck, M. P. Lynch and F. L. Wright, *J. Heterocycl. Chem.*, 1988, **25**, 555–558.
  - 8 M. Augustin, M. Koehler, J. Faust and M. M. Al-Holly, *Tetrahedron*, 1980, **36**, 1801–1805.
  - 9 *Antibase 2002, a database for rapid structure elucidation of microbial metabolites*, Wiley-VCH Verlag Berlin GmbH, Chemical Concepts Division, Weinheim, 2002.
  - 10 B. Clark, R. J. Capon, M. Stewart, E. Lacey, S. Tennant and J. H. Gill, *J. Nat. Prod.*, 2004, **67**, 1729–1731.